

Synthesis and photochemical properties of octacinnamoyl-substituted tetraazaporphyrins



H. Eichhorn,^a M. Rutloh,^b D. Wöhrle^{*,a} and J. Stumpe^b

^a Institut für Organische und Makromolekulare Chemie, Universität Bremen, Postfach 330440, 28334 Bremen, Germany

^b Institut für Organische Chemie, Humboldt-Universität zu Berlin, Eriseering 42, 10115 Berlin, Germany

New metal-free and metal-containing 2,3,7,8,12,13,17,18-octakis[(4-methoxycinnamoyl)oxyalkylthio]-tetraazaporphyrins with different polymethylene chain lengths (3, 6, 8 or 11 methylene groups) were synthesized by esterification of 2,3,7,8,12,13,17,18-octakis(hydroxyalkylthio)tetraazaporphyrins, obtained from 1,2-dicyano-1,2-bis(hydroxyalkylthio)ethylenes, with 4-methoxycinnamic acid. The structures of the compounds were confirmed by UV-VIS, IR, ¹H and ¹³C NMR spectroscopies. None of the derivatives shows liquid crystalline behaviour; their solid phase is of amorphous or microcrystalline consistency. On UV irradiation the dominating processes of the cinnamoyl groups are *E,Z* photoisomerization in solution and cross-linking reactions *via* the (C=C) bonds in spin-coated films, whereas photodegradation is the more (in solution) or less (in films) effective reaction of the tetraazaporphyrin chromophore. Further irradiation of the spin-coated films results in insoluble transparent films with a high content of tetraazaporphyrin moieties. All of the processes determined show a dependence upon the length of the polymethylene chains. The efficiency of the fluorescence, the photoisomerization and the cross-linking reactions of the cinnamoyl group are lower with decreasing chain length, whereas the photodegradation of the tetraazaporphyrin is increased. This contrary behaviour suggests the existence of energy-transfer processes from the cinnamoyl chromophore to the tetraazaporphyrin chromophore. In solution, the dependence of the efficiency on the distance with $1/R^6$ indicates a long-range dipole-dipole mechanism.

Introduction

Metal chelates, like porphyrins and phthalocyanines, are of great interest as materials for photovoltaic cells,¹ photoconductors and semiconductors,²⁻⁴ photocatalysts,⁵ phototherapeutic agents in the photodynamic therapy of cancer^{6,7} and active materials for optical data storage.⁸ Most of these properties are based on their interesting optical or photophysical properties.^{9,10} One promising approach in materials science is to combine specific molecular properties with supramolecular order. In this way, materials with anisotropic physical properties and the possibility of processing on a molecular level can be achieved. Examples of such supermolecular arrangements are self-organizing systems like liquid crystals or amphiphilic molecules.¹¹⁻¹³ A contrasting approach deals with an isotropic glassy morphology, producing non-scattering, optically transparent materials with additional good processing properties.¹⁴

Disc-like porphyrins like phthalocyanines or tetraazaporphyrins are known to readily arrange into stacks possessing nematic or columnar order. The columns themselves can form two-dimensional superlattices or columnar mesophases, which can be macroscopically aligned in films with anisotropic properties. The columnar order provides the opportunity for one-dimensional transport processes such as energy migration, electrical conductivity or photoconductivity.¹⁵⁻²⁰ On the other hand, monomeric glassy porphyrins are rarely described in the literature because of the strong tendency of the macrocycles to form ordered aggregates.¹⁴ However, such materials may be employed in investigating optical and photocatalytic properties.

For applications, thin films consisting of porphyrins in highly ordered or amorphous arrangements must be stabilized against the influence of solvents, *e.g.* thermal and mechanical stress. One possibility for stabilizing such films is by cross-linking. For

this reason, the introduction of cross-linkable groups in the periphery of the porphyrins is necessary. Cross-linking by irradiation is preferable to a thermally induced polymerization as it is temperature independent. The use of a photoinitiator for such a photocrosslinking has two disadvantages, however. An additional compound in the solid film is required and degradation products of the photoinitiator are formed, which may influence the structural order and physical properties. Light-induced cross-linking of cinnamic moieties by $[2\pi + 2\pi]$ photocycloaddition as the main process overcomes these disadvantages and is a well-known reaction in photopolymers.²¹

Cinnamoyl groups were also examined for the possibility of photocrosslinking molecules in their mesophase. Mertesdorf *et al.*²² and Kurihara *et al.*²³ described the photooligomerization of hexacinnamoyl-substituted azacrown and triphenylene derivatives, respectively, *via* the $[2\pi + 2\pi]$ photocycloaddition of the cinnamoyl group on UV irradiation. In the case of the azacrowns, the *E,Z* photoisomerization destroys the columnar ordered thermotropic mesophase and further light exposure results in isotropic cross-linked products. However, preformed columnar aggregates of the amphotropic derivatives could be photocrosslinked in non-polar solvents or in lyotropic mesophases. The photocycloaddition of the triphenylene derivatives is strongly depressed in their hexagonal solid state, D_{hd} mesophase and isotropic melt compared to the N_D mesophase. Within the temperature region of the N_D mesophase the conversion to oligomers decreases with increasing temperature. However, whether or not the mesophase was preserved during irradiation is not discussed.

The aim of this study was to investigate the thermotropic and photochemical behaviour of porphyrin derivatives containing substituents with C=C bonds. For that reason tetraazaporphyrins covalently connected to eight cinnamoyl groups *via* polymethylene chains of different lengths were investigated for

their thermal and photochemical properties. Tetraazaporphyrins were chosen due to their higher photochemical stability²⁴ compared to phthalocyanines and their low-intensity absorption at 310 nm, the wavelength region of the absorption of the cinnamic ester. Therefore, irradiation at *ca.* 310 nm should result in photocrosslinking. Furthermore, the disc-like structure of the tetraazaporphyrin offers potential mesogenic properties as known from metallated octakis(alkylthio)tetraazaporphyrins,¹⁵ but derivatives with functional groups in the side chain have not been investigated until now. Compared to the aforementioned azacrown and triphenylene derivatives, the octasubstituted tetraazaporphyrins are bichromophoric systems, in which the eight photochromic moieties are characterized by absorbance in the UV region, whereas the porphyrin core exhibits intense absorption in the visible region.

Results and discussion

Synthesis

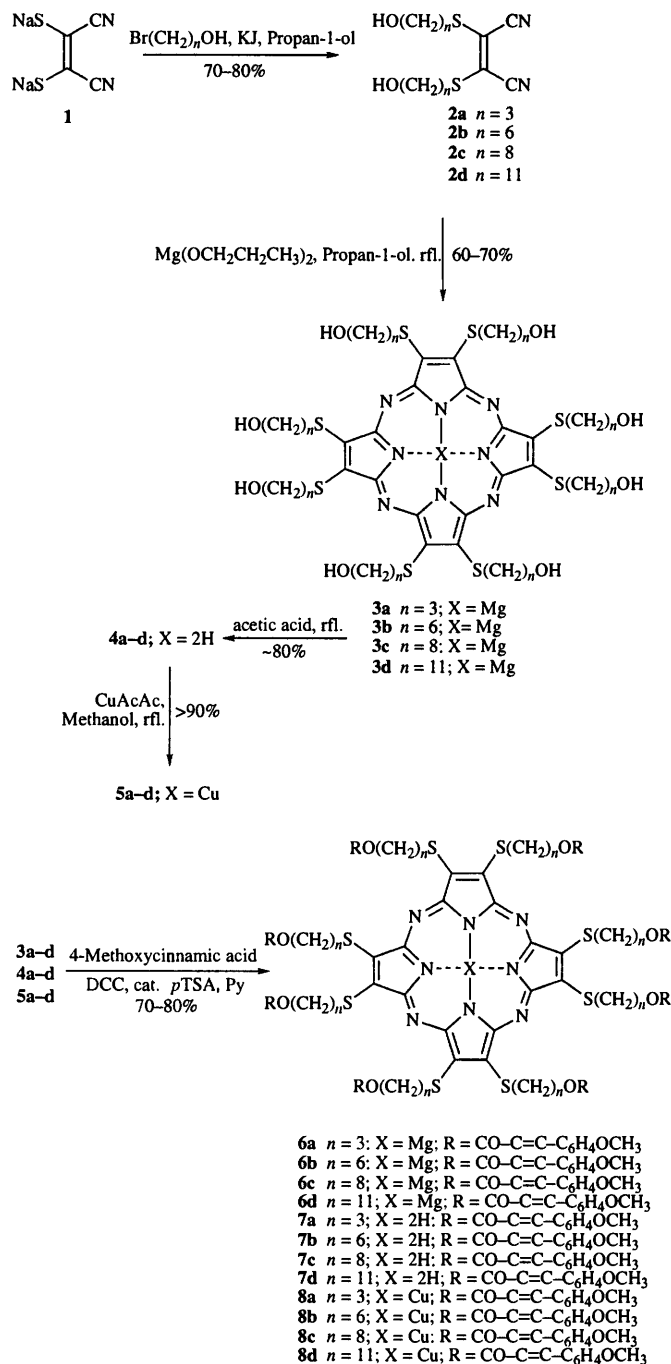
The readily available 1,2-dicyanoethylene-1,2-dithiolate **1** was employed as starting material for the preparation of tetraazaporphyrins having cinnamoyl groups covalently connected *via* spacers of differing length [(CH₂)_{*n*}, *n* = 3, 6, 8, 11]. **1** was reacted with bromoalkan-1-ols after a modified procedure of Schramm and Hoffman²⁵ giving yields of *ca.* 70% for the 1,2-dicyano-1,2-bis(hydroxyalkylthio)ethylenes (**2a–d**). The dinitriles **2a–d** were then cyclotetramerized in propan-1-ol to the magnesium octakis(hydroxyalkylthio)tetraazaporphyrins **3a–d** with magnesium powder, in yields of 60–70%. The yields of the substitution reaction of **1** and also the tetramerization of **2a–d** are not significantly influenced by the length of the polymethylene spacer. The magnesium chelates **3a–d** were converted into the metal-free tetraazaporphyrins **4a–d** in *ca.* 80% yield by heating **2a–d** in acetic acid at 80 °C.²⁶ Partly formed acetic ester groups were saponified in boiling methanolic potassium methanolate. Demetallation in sulfuric acid²⁵ or trifluoroacetic acid²⁷ led to yields of only < 50% of the metal-free derivatives. Compounds **4a–d** can be metallated by heating with metal salts in methanol as is shown in this work for the reaction with copper acetylacetonate with quantitative formation of **5a–d**.

It proved important to discover suitable reaction conditions for the quantitative esterification of the octahydroxy compounds **3a–d**, **4a–d** and **5a–d** with the (*E*)-4-methoxycinnamic acid giving **6a–d**, **7a–d** and **8a–d**. The best results were achieved by activation of the carboxylic acid group of the (*E*)-4-methoxycinnamic acid with dicyclohexylcarbodiimide in pyridine in the presence of toluene-*p*-sulfonic acid as catalyst.²⁸ All short chain compounds (*n* = 3, 6) could be esterified quantitatively, whereas for the long chain compounds (*n* = 8, 11) a small amount of the hepta-esterified product remained, as determined by IR and HPLC methods. These side products were separated by preparative HPLC.²⁹

NMR spectroscopy is the most valuable method for determining the composition of the dicyanoethylenes **2a–d** and the tetraazaporphyrins **3a–d**, **4a–d**, **6a–d** and **7a–d**. Tables 5–7 contain the ¹H and ¹³C NMR data. In all cases they are in agreement with values found for simple octa(alkylthio)-substituted tetraazaporphyrins^{15,27} and with theoretical calculations. The chemical shift of the resonance of the inner protons of the free base derivatives **4a–d** and **7a–d** depends on the solvent and in the case of **4a–d**, also on the length of the polymethylene chains. The ¹H NMR signals of the copper compounds **5a–d** and **8a–d** were very broad due to the paramagnetic copper ion. These compounds were therefore characterized by elemental analysis.

Thermal properties

Compounds **2**, **3** and **6** are highly viscous oils at room temperature, whereas compounds **4**, **5**, **7** and **8** precipitated as



solids. However, birefringent behaviour was not detectable for all compounds using polarizing microscopy, implying the solid materials are amorphous or microcrystalline. A more powerful method, differential scanning calorimetry (DSC), allowed characterization of the type of phase by the classification of phase transitions. In the first heating-run a melting transition, without discernible glass transitions, was detected for compounds **4b–d**, **5b–d**, **7b–d** and **8b–d**, whereas both transitions were found in the case of the short chain compounds **4a**, **5a**, **7a** and **8a**. In the second and also in subsequent heating all Mg^{II} tetraazaporphyrins as well as the metal-free and Cu^{II} derivatives **4a**, **5a,c**, **7a** and **8a,b** exhibited glass transitions without any indication of melting points (Table 1). For the copper chelates **5d** and **8c,d**, as well as for the metal-free compounds **4b–d** and **7b,d**, both a glass transition and a melting point were observed. In the case of **5b** and **7c** only melting points were observed. It should be noted that a storage period of six months at room temperature does not influence the thermograms.

Table 1 Transition temperatures of the compounds 2–8 determined by DSC

Sample	Transition temperatures/°C ($\Delta H/kJ mol^{-1}$)		Sample	Transition temperatures/°C ($\Delta H/kJ mol^{-1}$)	
	$K \rightarrow I^a$	$T_g^{a,b}$		$K \rightarrow I^a$	$T_g^{a,b}$
2a		-41	5c		58
2b		-60	5d	132 (51.5)	11
2c		-59	6a ^c		6.5
2d	18 (29.4)	-38	6b ^c		-1
3a		41	6c ^c		-21
3b		-7	6d ^c		-29
3c		-14	7a		25
3d		39	7b	79 (7.4)	4
4a		50 ^c	7c	73.5 (102.4)	
4b	104 (15.8)	41 ^c	7d	53 (55.3)	3
4c	73 (28.9)	-2	8a		28
4d	123 (42.7)	22	8b		2
5a		34	8c	65 (66.1)	-7
5b	79 (45.9)		8d	67, 75 (154.2)	-27

^a All transitions were observed during the second and subsequent heating runs. The heating rate was 10 K min⁻¹. ^b T_g means glass transition. ^c Very broad transition.

Table 2 Absorbance data of the compounds 3–8 in THF solution and in spin-coated films

Sample	λ_{max}/nm ($\epsilon/10^3 dm^3 mol^{-1} cm^{-1}$)		
	4-Methoxycinnamoyl ester	Octakis(alkylthio)tetraazaporphyrin	
		Sorêt-band	Q-bands
3a–d ^{a,b}		373 (51.0)	512 (10.5), 673 (50.5)
4a–d ^{a,b}		349 (44.1)	511 (20.8), 641 (26.0), 712 (34.1)
5a–d ^{a,b}		361 (41.0)	502 (14.6), 668 (52.5)
6a–d ^{a,b}	226 (114), 309 (193)	376 (51.0)	673 (49.0)
7a–d ^{a,b}	226 (118), 309 (194)	363 (50.0)	517 (23.0), 639 (29.0), 711 (38.0)
8a–d ^{a,b}	226 (134), 309 (199)	361 (48.0)	503 (17.0), 669 (59.0)
TAP ^{a,c}		375 (64.5)	509 (14.6), 672 (64.9)
Cinnamic ester ^{a,c}	227 (12.9), 308 (24.0)		
6a ^d	313	380	679
6b ^d	313	378	677
6d ^d	310	374	678
8a ^d	310	365	660
8d ^d	313	(360) ^e	690

^a Absorbance data in solution. ^b The length of the polymethylene chain has no significant influence on the spectroscopic behaviour. Therefore the derivatives a–d show the same values. Accuracy: λ_{max} , ± 1 nm; $\epsilon \pm 2\%$. ^c Absorption data of the compounds 2,3,7,8,12,13,17,18-octakis(butylthio)-5,10,15,20-tetraazaporphyrinatomagnesium (TAP) and (*E*)-4-methoxycinnamic ethyl ester (cinnamic ester) for comparison. ^d Absorbance data of spin-coated films on quartz. ^e Shoulder.

No thermotropic behaviour of compounds 2–8 was found by DSC and polarizing microscope investigations. Only compound 8d showed two adjacent peaks in the melting region, but birefringent behaviour could not be observed. These results are expected for compounds 6–8, caused by the eight rigid and bulky cinnamoyl groups at the end of the polymethylene chains. In the case of compounds 3–5 liquid crystalline properties are not disturbed by bulky moieties. Therefore, the potential of interaction of the terminal hydroxy groups seems to be reasonable. However, octa(hydroxyalkoxy)-substituted phthalocyanines have been reported to exist in columnar discotic phases.³⁰ These results are an indication of the expected larger mesogenic potential of phthalocyanines in comparison to tetraazaporphyrins.

It is concluded that the mesogenic behaviour and crystallization from the isotropic melt for all tetraazaporphyrins is disturbed by the hydroxy and the cinnamoyl substitution pattern. Furthermore, crystallization is influenced by the metal ion of the macrocycle and the length of alkylene chains. Magnesium disturbs the crystallization in comparison to the copper and metal-free derivatives. This may be as a result of the higher coordination number of magnesium in the macrocycles,

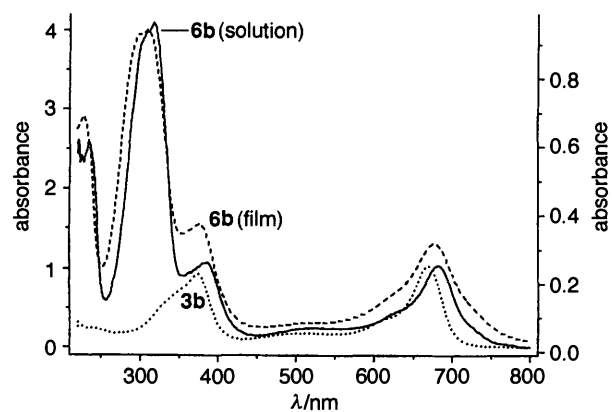


Fig. 1 Absorbance spectra of the compounds 3b, 6b in THF solution ($5 \times 10^{-6} mol l^{-1}$) (left axis) and 6b as spin-coated film (thickness 0.1 μm , right axis)

which may lead to axial interactions between magnesium and the oxygen of hydroxy or carbonyl groups, for example.

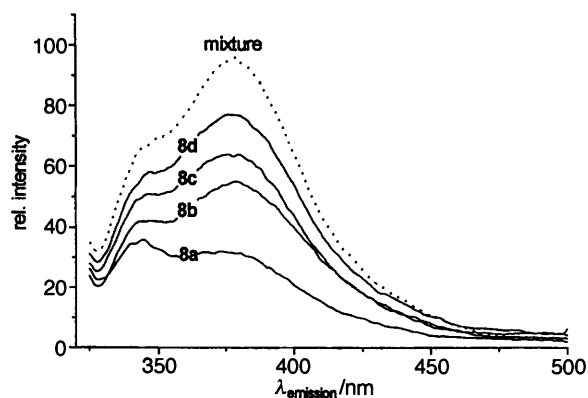


Fig. 2 Fluorescence spectra of **8a–d** (concentration 3.27×10^{-6} mol l^{-1}) and a mixture of copper octakis(methylthio)tetraazaporphyrin²³ with 4-methoxycinnamoyl ethyl ester⁴⁰ (molar ratio 1:8, concentration of the tetraazaporphyrin 3.27×10^{-6} mol l^{-1}) in THF. Excitation at 313 nm.

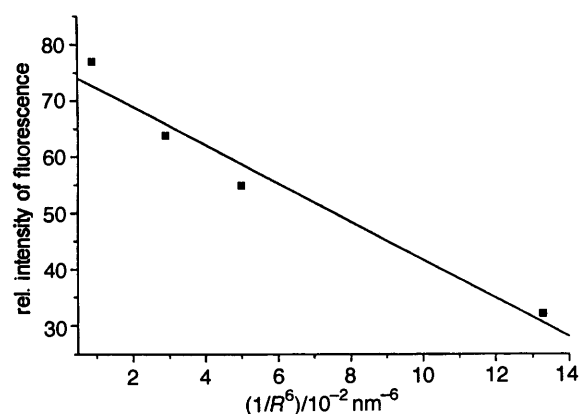


Fig. 3 Dependence of the fluorescence intensity ($\lambda_{ex} = 313$ nm) of **8a–d** (concentration 3.27×10^{-6} mol l^{-1}) in THF on the calculated distance R between the cinnamoyl groups and the tetraazaporphyrin moiety

Therefore, positional and orientational order in general and porphyrin–porphyrin interactions in particular are prevented. Decreasing the length of the polymethylene chains results in increasing glass transition temperatures and suppression of the recrystallization or microcrystallization of the side-groups in particular from the melt. In conclusion, all magnesium and the short chain copper as well as metal-free tetraazaporphyrin derivatives are amorphous materials.

Photochemistry in solution

The UV–VIS spectra of the octa(hydroxyalkylthio)tetraazaporphyrins **3–5** and the (*E*)-4-methoxycinnamic ester containing derivatives **6–8** are compared in Table 2 and selected examples are shown in Fig. 1. The spectra of **3–5** with intense Q- and Soret-band transitions are comparable to the spectra of octa(alkylthio)tetraazaporphyrins.^{15,27} Derivatives **4** and **7** exhibit the characteristic splitting of the Q-band caused by the D_{2h} symmetry of the metal-free macrocycle. The tetraazaporphyrins **6–8** show in addition the maxima of absorbance of the cinnamoyl chromophore at 226 and 309 nm. Considering the 8:1 molar ratio of cinnamic ester groups and the tetraazaporphyrin macrocycle in **6–8**, the absorbance of the chromophores were approximately additive compared to those of (*E*)-4-methoxycinnamic ethyl ester and **3–5**. Therefore, no significant intra- or inter-molecular interactions between the ground states of the covalently linked chromophores exist in dilute solutions of tetrahydrofuran (THF) and toluene as solvents.

In contrast, the fluorescence behaviour of the three series of linked bichromophoric derivatives **6–8** indicates an intramolecu-

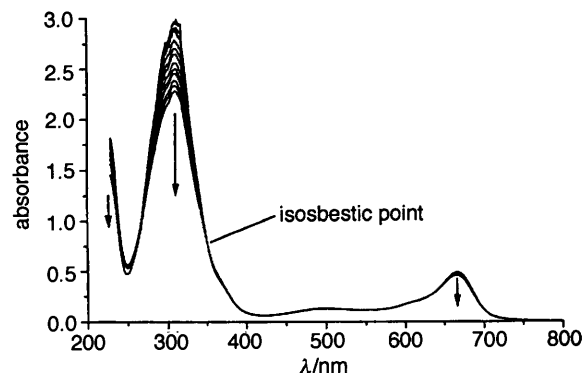


Fig. 4 Change of UV–VIS spectra of **8d** (concentration 1.6×10^{-5} mol l^{-1}) in THF on irradiation at 313 nm with 3 mW cm^{-2} . Irradiation time 0–600 s. Measurements under inert gas.

lar interaction between the excited cinnamic esters and the central tetraazaporphyrin (Figs. 2, 3). In dilute solutions of THF, the exposure at 313 nm causes an excitation of the cinnamoyl moieties, which results in a weak, broad fluorescence band with a maximum at 375 and a shoulder at 340 nm. Similar fluorescence emissions were observed for cinnamic esters in the side-chains of polymers in chloroform solutions.^{31–33} The emission intensities of the cinnamic esters of **6–8** is strongly dependent on the length of the polymethylene chain (this also means the distance) between the primary excited cinnamoyl chromophores and the central tetraazaporphyrin moiety. The intensity decreases as follows: (*E*)-4-methoxycinnamic ethyl ester > 8:1 mixture of (*E*)-4-methoxycinnamic ethyl ester and copper-octakis(methylthio)tetraazaporphyrin > **6–8d** > **6–8c** > **6–8b** > **6–8a**. The decrease is approximately linear in $1/R^6$, if R is the average intramolecular distance between the cinnamoyl groups and the tetraazaporphyrin moiety (Fig. 3). Physical mixtures of (*E*)-4-methoxycinnamic ethyl ester and octa(alkylthio)tetraazaporphyrins, identical in concentration and molar ratio of 8:1, show a higher fluorescence intensity compared to the covalently bound compounds. In conclusion, this characteristic dependence of the interchromophoric distance, the overlapping of the cinnamic ester emission band and the tetraazaporphyrin Soret-band absorption as well as the intramolecular distance between approx. 5 and 22 nm from the cinnamic ester to the tetraazaporphyrin suggest a 'Förster' (dipole–dipole) mechanism of energy transfer.³⁴

Fluorescence of the thio-substituted tetraazaporphyrins **3–8** was not observed (by excitation either in the Q- or Soret-band region), whereas unsubstituted and octaalkyl-substituted tetraazaporphyrins exhibit a fluorescence; 5–10 nm red shifted to the Q-band absorption.³⁵ This missing fluorescence is probably caused by a typical heavy atom effect of the sulfur atoms in the tetraazaporphyrins **3–8**.

Irradiation of cinnamic esters in solution is well known to result in *E,Z* photoisomerization and, depending on concentration, in $[2\pi + 2\pi]$ photocycloaddition of the double bond,^{22,36,37} whereas the irradiation of the tetraazaporphyrin effects a decomposition of the macrocycle.²⁴ Thus, irradiation of the tetraazaporphyrin derivatives **6–8** dissolved in THF or toluene at $\lambda = 313$ nm results in three different UV–VIS spectroscopically observable processes (Fig. 4). Following the absorption band of the cinnamoyl group at 313 nm, a fast decrease of the absorbance is observed at first which becomes a much slower decrease after ca. 500 s (Fig. 5). As the third process, a slow decrease of the Q-band of the tetraazaporphyrin at 665 nm (metallated derivatives) or 710 nm (metal-free derivatives) was observed following first-order kinetics.

The fast process at 313 nm is due to the photoisomerization of the *E*- to the *Z*-isomer, since the latter has a smaller absorption coefficient. The observed isosbestic point at 350 nm (332 nm in the case of Mg-derivatives **6**) and the straight lines of

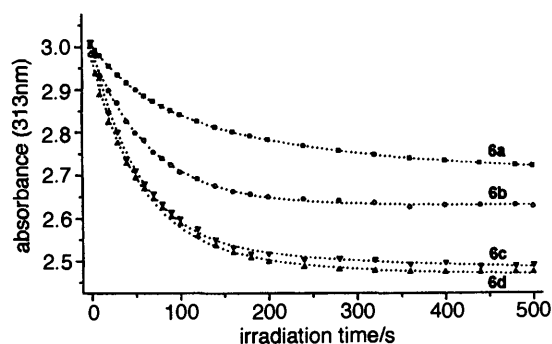


Fig. 5 Change of the absorbance of **6a–d** (concentration 1.6×10^{-5} mol l^{-1}) in THF at 313 nm on irradiation at 313 nm with 3 mW cm^{-2} in dependence on the irradiation time. Measurements under inert gas.

Table 3 Quantum yields of the *E,Z* photoisomerization and ratio of the isomers in the photostationary state of cinnamic esters in 1.24×10^{-4} mol dm^{-3} solutions related to the cinnamoyl groups

Sample	$\phi_{313}^{E \rightarrow Z}$	$\phi_{313}^{Z \rightarrow E}$	$[E]_{\text{ps}}/[Z]_{\text{ps}}^a$
6a^b	0.04	0.16	2.3
6b^b	0.10	0.26	1.7
6c^b	0.17	0.21	0.8
6d^b	0.21	0.25	0.8
7a^c	0.01	0.02	2.4
7b^c	0.03	0.03	1.3
7c^c	0.05	0.04	1.3
7d^c	0.05	0.04	1.1
8a^c	0.01	0.02	2.3
8b^c	0.02	0.02	1.2
8c^c	0.05	0.03	1.1
8d^c	0.06	0.04	1.0

^a Molar ratio of the *E*- and *Z*-isomer in the photostationary state. ^b Solvent THF. ^c Solvent toluene.

the absorption diagrams³⁸ suggest that the photoreaction is spectroscopically uniform in the initial period at *ca.* 300 s. Therefore, the quantum yields of the *E* \rightarrow *Z* photoisomerization could be determined by the method of initial slopes as described by Lippert and Lüder.³⁹ Using these *E* \rightarrow *Z* quantum yields, the quantum yields of the *Z* \rightarrow *E* photoisomerization were calculated from the fractions of the two isomers at the photostationary state (see Experimental and Table 3).

In the polar solvent THF, higher quantum yields for the isomerization and higher molar ratios of *Z*-isomers in the photostationary state were obtained in comparison to the less polar toluene. This solvent effect of cinnamic ester has been described previously.³⁷ However, the sum of the quantum yields is less than one in each case. In both solvents the molar ratio of *E/Z* isomers in the photostationary state decreases with increasing number of methylene groups, which is 0.53 for the cinnamic ethyl ester (Table 3). This observation is explained as resulting from steric hindrance of the more bulky *Z*-isomer in the closely packed arrangement of compounds **6–8**. The hindrance is more distinct in the case of short polymethylene chains compared to longer ones. For the short chain compounds **6a**, **7a**, **8a**, 5.6 of the eight cinnamoyl groups exists statistically as the *E*-isomer, whereas for the long chain compounds **6d**, **7d**, **8d** only 3.5 cinnamoyl groups have the *E* configuration in the steady-state. Steric hindrance of the formation of the *Z*-isomer was also shown for the *E,Z*-isomerization of cinnamic ethyl esters in the smectic phase of a liquid crystalline guest–host system compared to the isotropic state.⁴⁰

The quantum yields of *E* \rightarrow *Z* and *Z* \rightarrow *E* photoisomerization decrease with decreasing number of methylene groups in the alkylene chains. Also, a stronger dependence on the distance

Table 4 Stability of the tetraazaporphyrins under different conditions by irradiation at 313 nm in solution and as spin-coated film

Sample (Concentration)	Solvent	$k/10^3 \text{ min}^{-1}$	Decomposition at $t = 100 \text{ min}$ (%)
6a^a	THF	5.9	45
6b^a	THF	4.2	34
6c^a	THF	2.1	19
6d^a	THF	1.6	15
8d^a	THF	1.6	15
7a–8d^b	Toluene	<i>ca.</i> 0.2	2

Sample (films of around 100 nm thickness) ^b	$t_{1/20}/\text{min}^c$	$t_{1/10}/\text{min}^c$	Decomposition at $t = 100 \text{ min}$ (%)
6a	11	32	17
6b	18	51	15
6d	44	—	9
8a	5	18	21
8d	21	55	16

^a Measurements under argon, concentration $16 \mu\text{mol dm}^{-3}$. ^b Measurements in air, concentration $16 \mu\text{mol dm}^{-3}$. ^c Decrease of the absorbance at 670 nm of 5 or 10%.

to the tetraazaporphyrin core is given for the *E* \rightarrow *Z* process in comparison to the *Z* \rightarrow *E* isomerization (Table 3). With regard to the excited *E* and *Z* isomers, there is sufficient agreement with the fluorescence quenching of the *E*-cinnamoyl chromophores.

Like the second process, a very slow additional decrease of the absorption at 313 nm is seen after *ca.* 500 s for compounds **6–8** (Fig. 5). This process may be caused by the $[2\pi + 2\pi]$ photocycloaddition of the cinnamoyl groups. The quantum yields of this process were between 10^{-3} and 10^{-5} and comparable with the values found for the $[2 + 2]$ photocycloaddition of cinnamic ethyl ester in dilute ethanol solutions.⁴¹ Since no intermolecular crosslinked products with higher molecular mass were detected by gel-permeation chromatography (GPC), this process should occur intramolecularly between neighbouring double bonds. Such a concentration-independent intramolecular photocycloaddition was established in dilute solutions of dicinnamic esters.⁴² Later it will be shown that intermolecular crosslinking is the predominant process in the solid state.

The third observed process in solution under irradiation at 313 nm is a slow photodegradation of the tetraazaporphyrin (Fig. 4). The stability of the macrocycle was determined by the decay of Q-band absorption. As described by Sobbi *et al.*²⁴ for phthalocyanines the rate of the decay is of first-order kinetics with respect to the porphyrin concentration. Table 4 shows the values of the rate constants k and half-lives. In contrast to THF, the stability of all tetraazaporphyrins in toluene solution is much higher (see Table 4 for selected examples for **7a–d** and **8a–d**). After 10 h irradiation differences in the decreasing rate were not observable. For **6a–d** it is shown that a decreasing number of methylene groups effect an increase of the photodecomposition of tetraazaporphyrin. The opposite efficiencies of fluorescence and photoreactions of the connected (*E*)-cinnamic ester on the one hand and the photodegradation of the tetraazaporphyrin moiety on the other, are strong indications for the postulated intramolecular energy-transfer mechanism.

Photochemistry in the solid state

The photocycloaddition and photoisomerization processes of cinnamic esters are strongly influenced by their order and mobility in the solid state. This was recently described for amorphous, liquid crystalline, crystalline, host–guest and polymeric systems containing cinnamoyl groups.^{21,36,40,43–45}

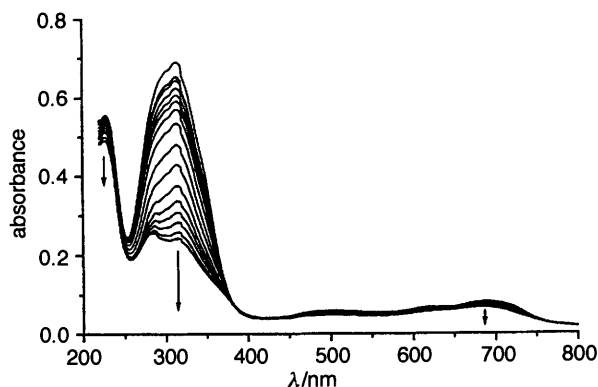


Fig. 6 Change of UV-VIS spectra of a spin-coated film of **8d** on irradiation at 313 nm with 3 mW cm^{-2} . Irradiation time 0–6000 s.

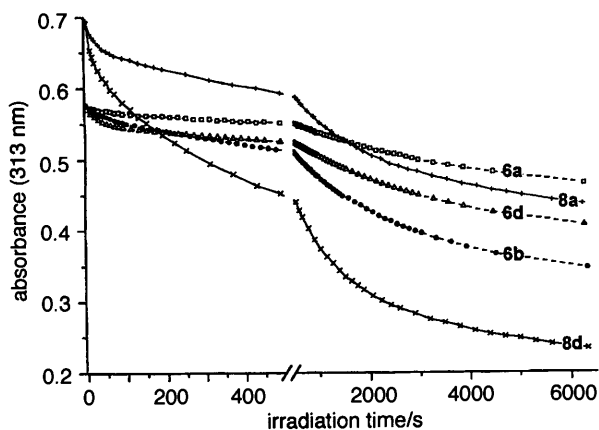


Fig. 7 Change of the absorbance at 313 nm of **6a, b, d, 8a** and **8d** as spin-coated films on irradiation at 313 nm with 3 mW cm^{-2} in dependence on the irradiation time

At room temperature, preheated films of the octacinnamoyl-substituted tetraazaporphyrins are optically transparent, do not scatter light nor are birefringent, suggesting that they are amorphous or microcrystalline as previously described. The absorption spectra of these films are comparable to those obtained in solution (Table 2, Fig. 1). This, in addition to the glass transitions in the DSC thermograms, is an indication of the weak interaction of the tetraazaporphyrin moiety in the solid state. Only the copper derivative **8d** exhibits a small bathochromic shift of the Q-bands, accompanied by broadening of the band.

Spin-coated films of the derivatives **6a, b, d** and **8a, d** were investigated on irradiation at 313 nm with 3 mW cm^{-2} . The absorption of the cinnamoyl groups first shows a rapid decrease during an initial period of *ca.* 100 s and then passes to a slower, continuous decrease over the measuring time of 6000 s (Figs. 6, 7). Also, in the FTIR spectra, a reaction of the C=C bonds was implied by a decrease in the $\nu_{\text{C=C}}$ absorption at 1635 cm^{-1} .

After an irradiation time of not more than 1200 s the resulting films became completely insoluble in organic solvents. Insoluble parts were first observed after *ca.* 300 s, therefore, the photoprocesses in the films are dominated by intermolecular photocrosslinking of the cinnamoyl groups. The conversion rates of the cinnamoyl groups were spectroscopically determined at an irradiation time of 6000 s. For the films of compounds **6a, 6b, 6d, 8a** values of 30–60% have been observed, whereas in the case of **8d** a rate of *ca.* 75% was found (Fig. 7). The very high conversion rate of **8d** can be explained by the microcrystalline morphology of the film. An indication for this was the decreased conversion rate (to 40%) of analogous films

of **8d** irradiated at 65°C , the melting range of the compound in the DSC thermogram. Insoluble films were always obtained by 10% conversion of the cinnamoyl groups.

The photoreactions in the films may consist of [2 + 2] photocycloaddition, polymerization and *E,Z* photoisomerization. Eggerton *et al.* established all three photoreactions in films of polymers containing cinnamoyl groups in the side-chains.²¹ Their photoproducts contain *ca.* 65% cyclodimers and the remaining part as oligomers. The *E,Z* photoisomerization occurs only as a negligible aspect of the photoreactions.

Comparable to the results found for solutions, the tetraazaporphyrin moieties undergo degradation when the films are irradiated at 313 nm in air. The compounds are more stable in the films than in THF solutions under an inert atmosphere and less stable compared to the solutions in toluene under air (see Table 4). After an irradiation time of 1200 s, sufficient for complete crosslinking, around 2–10% decomposition of the macrocycle was observed.

Both processes, the photoreaction of the C=C bonds and the decomposition of the macrocycle (see Fig. 7 and Table 4), depend on the spacer length in a similar way to that described previously for solutions. Thus, the consumption rate of the C=C bonds increases and the decomposition rate of the macrocycle decreases with increasing spacer length. These results also suggest an intramolecular energy transfer from the cinnamoyl donor to the tetraazaporphyrin acceptor in the solid state. The correlation of both processes is not as good as in solution. This is explainable by the additional influence of the film morphology on the topochemically controlled bimolecular reaction and the energy transfer.

Conclusion

The disc-like tetraazaporphyrins **6–8** functionalized with photoactive 4-methoxycinnamoyl moieties at the end of their eight side groups are not liquid crystalline. Also, their tendency to crystallize is strongly depressed and, for this reason, clear, amorphous films can be prepared by spin-coating. On UV irradiation the films are photocrosslinked by the $[2\pi + 2\pi]$ photocycloaddition and polymerization of the C=C bonds of the cinnamoyl groups, which is the dominating photoprocess. Under these conditions the photochemical decomposition of the tetraazaporphyrin cores take place as a minor side-reaction (<2%). Thus, the procedure results in insoluble transparent polymeric films with a high content of tetraazaporphyrin chromophores (up to 26 mass%).

In solution, the *E,Z* photoisomerization of the cinnamoyl groups is the dominant process on UV irradiation, whereas a small amount of intramolecular photocycloaddition of the cinnamoyl moieties and photodecomposition of the tetraazaporphyrin take place as side reactions. However, the photophysical and photochemical behaviour of the multichromophoric molecules depend strongly on the length of the alkyl chains between the central core and the cinnamoyl groups. Thus, the quantum yields of the fluorescence, the *E,Z* photoisomerization and the photocycloaddition of the cinnamoyl groups are lowered with a decreasing number of methylene groups, while simultaneously, the efficiency of the photodecomposition of the tetraazaporphyrin moiety increases. Therefore, an efficient intramolecular energy-transfer process from the S_1 state of the cinnamoyl moiety as donor to the tetraazaporphyrin acceptor is proposed. The linear correlation between the fluorescence intensity and the calculated distance between both chromophores with $1/R^6$ suggests a long-range dipole-dipole mechanism for the transfer process.

For creating a mesogenic porphyrazine, the integration of the cinnamoyl moieties into the disc-shaped porphyrazine core is a more promising molecular design, but from the photochemical point of view, a sufficient distance between both these chromophores is necessary. Therefore, other types of chromophores have to be combined for success.

Experimental

Materials

All commercially available chemicals were of analytical grade. Tetrahydrofuran (THF) was carefully purified from 1,6-di-*tert*-butyl-4-methylphenol by distillation over KOH under inert gas. All other solvents were dried over molecular sieves and used without further purification. For flash chromatography Matrix Silica Si chromatography medium (60 Å 35–70 µm particle size), a product of Amicon (Witten, Germany), or RP-18 material from Merck (LiChroprep RP-18, 25–40 µm) was used. TLC was carried out using Macherey–Nagel's (Düren, Germany) Polygram 0.25 mm SIL G/UV₂₅₄ pre-coated plastic sheets. Optically clear films of the tetraazaporphyrin derivatives were obtained by spin-coating. 200 µl of a 50 mmol l⁻¹ tetraazaporphyrin solution in THF was spread on a rotating rectangular glass substrate (2.5 × 1 cm). The obtained film was heated at 80 °C to remove the solvent. Layer thicknesses of ca. 100 nm were determined with a Sloan Dektak II.

Instrumentation

For analysis the following instruments were used: UV–VIS absorption spectra with a Perkin-Elmer Lambda 9, FTIR spectra with a Bio-Rad Digilab FTIR FTS7 instrument, fluorescence spectra with a Perkin-Elmer LD50 spectrometer, ¹H and ¹³C NMR spectra with a Bruker WH 360 spectrometer (using the deuterium signal of the solvent as the lock and SiMe₄ as internal standard). The HPLC chromatograms were recorded with a Merck-Hitachi-System (L-3000 Photo Diode Array Detector, L-6200A Intelligent Pump, T-6300 Column Thermostat, AS 2000A Autosampler). As the column, a Merck LiChrospher Si-60 (5 µm) with 250 mm length and 4 mm inner diameter was used. The DSC-measurements were carried out on a Polymer Laboratories DSC with an Auto-Cool-System. A polarizing-microscope (Leitz, Wetzlar) with hot stage was used for optical investigations.

Photochemical measurements

Measurements were carried out in a quartz cell (1 × 1 cm) at 30 °C. Typically, 3 ml of a solution of known concentration of a tetraazaporphyrin derivative was used. The measurements in THF were carried out under inert gas (three pump and freeze cycles) and in toluene under air. The irradiation was carried out using a high-pressure mercury lamp (HBO 500, Narva Berlin) as radiation source. The light was collimated using a quartz lens, passed through a water filter and a metal-interference filter (313 nm). All components were mounted on an optical bench. The absorption behaviour in dependence on irradiation was measured using a UV–VIS spectrometer (Perkin-Elmer Lambda 19). The light intensity was determined quantitatively by a potassium tris(oxalato)ferrate(III) actinometer. The light intensity was adjusted to 3 mW cm⁻² (4.73 × 10¹⁵ photons cm⁻² s⁻¹). Similar irradiation of spin-coated films on quartz were irradiated under comparable conditions.

Calculations of the quantum yields and the efficiencies of the photoreactions

The absorption–time curves of the reversible photoisomerization could be correlated according to eqn. (1), where $n = 1$

$$A = f(c, t) = b + \sum_{i=0}^n a_{(2i+1)} e^{(-a_{(2i+1)}t)} \quad (1)$$

(A : absorption, c : concentration, t : time, a : kinetic coefficients, b : constant)

for the solutions of compounds **6–8** with additional cycloaddition. The observed correlation rates r were >0.99. The artificial values of dA/dt for $t = 0$ were calculated using the adapted functions of eqn. (1). Then the quantum yields $\phi_{313}^{E \rightarrow Z}$ of

the $E \rightarrow Z$ photoisomerizations were calculated from eqn. (2),^{39,46} where $I_{\text{abs},313}^E$ is the light intensity absorbed by the E -

$$\phi_{313}^{E \rightarrow Z} = \frac{dA_{313}}{dt} \frac{V}{(\epsilon_{313}^E - \epsilon_{313}^Z) X I_{\text{abs},313}^E} \Big|_{t=0} \quad (2)$$

isomer of the cinnamoyl groups at 313 nm, ϵ_{313}^E and ϵ_{313}^Z are the extinction coefficients of the E - and Z -isomers at 313 nm, X is the optical path length, V is the irradiated reaction volume and A_{313} is the absorption of the reaction solution at 313 nm.

$I_{\text{abs},313}^E$ was calculated according to eqn. (3), where $[E]$ is the

$$\frac{I_{\text{abs},313}^E}{V} = \frac{\epsilon_{313}^E [E] I}{A} (1 - 10^{-A}) \quad (3)$$

concentration of the E -isomer and I the incident photons in mol s⁻¹.

With $\phi_{313}^{Z \rightarrow E}$ the quantum yield of the $Z \rightarrow E$ isomerization $\phi_{313}^{Z \rightarrow E}$ can be calculated from eqn. (4), where $[Z]_{\text{pss}}$ and $[E]_{\text{pss}}$

$$\frac{[Z]_{\text{pss}}}{[E]_{\text{pss}}} = \frac{\phi_{313}^{E \rightarrow Z} \epsilon_{313}^E}{\phi_{313}^{Z \rightarrow E} \epsilon_{313}^Z} \quad (4)$$

are the concentrations of the E - and Z -isomer in the photostationary state.

The aforementioned calculations include a few basic requirements. To determine the absorption coefficient of the Z -isomer, a dilute THF or toluene solution of (E)-4-methoxycinnamic ethyl ester was irradiated under identical conditions. Then the unknown isomer fraction of the photostationary state was determined by ¹H NMR spectroscopy and the absorption coefficient of the Z -isomer was calculated: $\epsilon_{313}(E\text{-isomer}) = 21\,100$ (20 000) and $\epsilon_{313}(Z\text{-isomer}) = 13\,800$ (13 600) in THF (toluene) solution. Therefore, the absorption coefficients at 313 nm of the reference compounds, 4-methoxycinnamic ethyl ester (E - and Z -isomer) and octa(alkylthio)tetraazaporphyrin, should be unchanged in compounds **6–8**. The change of the absorption at 313 nm due to other reactions, e.g. photocycloadditions or photodegradations, have to be negligible in the starting period of the isomerization. Furthermore, a thermal $Z \rightarrow E$ isomerization was not observed. The experimental error of the quantum yields for the solutions of compounds **6–8** was calculated to be ±5%, due to the error for the determination of the absorbance in the photostationary state.

The efficiency of the photodegradation of the tetraazaporphyrins in solution was determined from the slope of the lines in the first-order plots as described by Sobbi *et al.*²⁴ It was proved for all substances that there is no photoproduct absorbing in the spectral range 600–750 nm.

Disodium 1,2-dicyanoethylene-1,2-dithiolate 1

The compound was prepared by the method of Davison and Holm.⁴⁷ The UV–VIS and FTIR spectra agreed with the reported spectra in the literature.

1,2-Dicyano-1,2-bis(hydroxyalkylthio)ethylenes 2a–d

Compounds with different chain length [(CH₂) _{n} , $n = 3, 6, 8, 11$] were obtained by a modified procedure of Schram and Hoffman.²⁵ To a vigorously stirred suspension of **1** (20 mmol, 3.72 g) and sodium iodide (2 mmol, 300 mg) in propan-1-ol (50 ml) solutions of bromoalkan-1-ol (39 mmol) in propan-1-ol (10 ml) were added dropwise. After 48 h the solvent was evaporated in vacuum and the brown, oily residues were extracted with dry, hot *tert*-butyl methyl ether until colourless. After evaporating the ether in vacuum, red–brown, highly viscous products were obtained. For analytical measurements 100 mg of the products were purified by column chromatography on RP-18 using propan-2-ol–water 6:4 as eluent.

1,2-Dicyano-1,2-bis(3-hydroxypropylthio)ethylene 2a. (Yield

Table 5 ^1H NMR data of the compounds **2–4** (δ ; 360 MHz; Me_2SO)

Compound	<i>n</i>	(2 H, t, OH)	(4 H, t, O-CH ₂)	(4 H, m, S-CH ₂)	(4 H, m, CH ₂)	(4 × { <i>n</i> - 3} H, m, CH ₂)	(2 H, s, NH)
2a	3	4.7	3.5	3.2	1.8	—	
2b	6	4.7	3.4	3.2	1.7	1.5–1.2	
2c	8	4.7	3.4	3.15	1.65	1.4–1.2	
2d	11	4.7	3.3	3.1	1.6	1.4–1.2	
3a	3	4.55	3.6	4.1	1.9	—	
3b	6	4.25	3.2	4.05	1.75	1.5, 1.2–1.1	
3c	8	4.2	3.2	4.0	1.7	1.45, 1.2–1.0	
3d	11	4.2	3.2	4.0	1.7	1.4, 1.2–0.8	
4a	3	4.55	3.6	4.0	1.95	—	–2.05
4b	6	4.2	3.2	3.85	1.7	1.5, 1.2–1.1	–2.4
4c	8	4.2	3.2	3.8	1.7	1.45, 1.2–1.0	–3.1
4d ^a	11	3.8 ^b	3.3	4.1	1.9	1.6, 1.4–1.1	— ^c

^a Measurement at 100 °C with a 200 MHz spectrometer. ^b Very broad. ^c Measurement not below –2.5 ppm.

Table 6 ^{13}C NMR data of the compounds **2–4** (δ ; 360 MHz; Me_2SO)

Compound	<i>n</i>	(C=C)	(CN)	(O-CH ₂)	(S-CH ₂)	(CH ₂) _{<i>n</i>-2}
2a	3	121.1	112.4	58.6	32.3	31.5
2b	6	120.6	111.7	61.5	34.5	31.9, 29.35, 27.7, 24.7
2c	8	120.7	111.8	62.0	34.7	32.25, 29.5, 28.8, 28.6, 27.95, 25.3
2d	11	121.0	112.3	60.7	34.4	32.6, 29.5, 29.1, 29.0, 28.98, 28.9, 28.4, 27.7, 25.5
3a	3	140.3	156.6	59.4	33.4	31.2
3b	6	140.1	156.6	60.6	34.3	32.4, 30.1, 28.2, 25.1
3c	8	140.1	156.6	60.6	34.3	32.5, 30.1, 28.9, 28.8, 28.3, 25.4
3d	11	140.0	156.5	60.6	34.2	32.5, 30.0, 29.0, 28.9, 28.8, 28.6, 28.1, 25.5, 25.4
4a	3	139.6	152.0	59.4	33.2	31.1
4b	6	138.0	151.5	60.6	34.2	32.5, 30.0, 28.4, 25.3
4c	8	138.0	151.5	60.7	34.0	32.5, 29.7, 28.8, 28.6, 25.6, 25.4
4d						Too low solubility

3.77 g, 73%), $\lambda_{\text{max}}(\text{EtOH})/\text{nm}$ 212 ($\epsilon/\text{dm}^3 \text{ mol}^{-1} \text{ cm}^{-1}$ 5800), 275 (4600), 341 (14 500); $\nu_{\text{max}}/\text{cm}^{-1}$ 3400br (OH), 2939 and 2882 (CH), 2212 (CN), 1654br (C=C), 1052 (C–OH); *m/z* (FAB, glycerine) 257 (M – H⁺, 61%), 199 [M – (CH₂)₃OH, 100%], 140 [M – 2(CH₂)₃OH, 41%].

1,2-Dicyano-1,2-bis(6-hydroxyhexylthio)ethylene 2b. (Yield 4.79 g, 70%), $\lambda_{\text{max}}(\text{EtOH})/\text{nm}$ 212 ($\epsilon/\text{dm}^3 \text{ mol}^{-1} \text{ cm}^{-1}$ 5800), 275 (4600), 341 (14 500); $\nu_{\text{max}}/\text{cm}^{-1}$ 3400br (OH), 2932 and 2859 (CH), 2210 (CN), 1656br (C=C), 1050 (C–OH); *m/z* (FAB, glycerin) 341 (M – H⁺, 2%), 241 [M – (CH₂)₃OH, 100%], 140 [M – 2(CH₂)₆OH, 56%].

1,2-Dicyano-1,2-bis(8-hydroxyoctylthio)ethylene 2c. (Yield 5.98 g, 75%), $\lambda_{\text{max}}(\text{EtOH})/\text{nm}$ 212 ($\epsilon/\text{dm}^3 \text{ mol}^{-1} \text{ cm}^{-1}$ 5800), 275 (4600), 341 (14 500); $\nu_{\text{max}}/\text{cm}^{-1}$ 3427br (OH), 2928 and 2856 (CH), 2210 (CN), 1654br (C=C), 1051 (C–OH); *m/z* (FAB, glycerin) 397 (M – H⁺, 7%), 269 [M – (CH₂)₈OH, 100%], 140 [M – 2(CH₂)₈OH, 65%].

1,2-dicyano-1,2-bis(11-hydroxyundecylthio)ethylene 2d. (Yield 6.56 g, 68%), $\lambda_{\text{max}}(\text{EtOH})/\text{nm}$ 212 ($\epsilon/\text{dm}^3 \text{ mol}^{-1} \text{ cm}^{-1}$ 5800), 275 (4600), 341 (14 500); $\nu_{\text{max}}/\text{cm}^{-1}$ 3365br (OH), 2930 and 2854 (CH), 2210 (CN), 1655br (C=C), 1057 (C–OH); *m/z* (FAB, glycerin) 481 (M – H⁺, 1%), 311 [M – (CH₂)₁₁OH, 13%].

^1H and ^{13}C NMR data are given in Tables 5 and 6. The thermotropic behaviour is shown in Table 1.

Magnesium 2,3,7,8,12,13,17,18-octakis(hydroxyalkylthio)-5,10,15,20-tetraazaporphyrinato **3a–d**

Mg powder (486 mg, 20 mmol) was refluxed overnight in dry 150 ml propan-1-ol. **2a–d** (30 mmol) were added, and the suspension was refluxed with stirring for 36 h. The resulting blue suspensions were hot filtered, and the residues were washed with propan-1-ol. The solvent from the collected extracts was evaporated and the residues were refluxed with 100 ml 10% aqueous Na₂CO₃ solution. The suspensions were centrifuged and washed intensively with distilled water. The blue, highly viscous products were purified by chromatography

on RP-18 using as eluent propan-2-ol–water 7:3 in the case of **3a**, 8/2 for **3b–c** and 9/1 for **3d**.

3a. (Yield 5.71 g, 72%), $\lambda_{\text{max}}(\text{THF})/\text{nm}$ 373 ($\epsilon/\text{dm}^3 \text{ mol}^{-1} \text{ cm}^{-1}$ 51 000), 512 (10 500), 673 (50 500); $\nu_{\text{max}}/\text{cm}^{-1}$ 3330br (OH), 2929 and 2876 (CH), 1052 (C–OH), 1021.

3b. (Yield 7.10 g, 68%), $\lambda_{\text{max}}(\text{THF})/\text{nm}$ 373 ($\epsilon/\text{dm}^3 \text{ mol}^{-1} \text{ cm}^{-1}$ 51 000), 512 (10 500), 673 (50 500); $\nu_{\text{max}}/\text{cm}^{-1}$ 3330br (OH), 2931 and 2856 (CH), 1050 (C–OH), 1029.

3c. (Yield 8.48 g, 70%), $\lambda_{\text{max}}(\text{THF})/\text{nm}$ 373 ($\epsilon/\text{dm}^3 \text{ mol}^{-1} \text{ cm}^{-1}$ 51 000), 512 (10 500), 673 (50 500); $\nu_{\text{max}}/\text{cm}^{-1}$ 3340br (OH), 2930 and 2854 (CH), 1051 (C–OH), 1029.

3d. (Yield 8.79 g, 60%), $\lambda_{\text{max}}(\text{THF})/\text{nm}$ 373 ($\epsilon/\text{dm}^3 \text{ mol}^{-1} \text{ cm}^{-1}$ 51 000), 512 (10 500), 673 (50 500); $\nu_{\text{max}}/\text{cm}^{-1}$ 3366br (OH), 2926 and 2851 (CH), 1049 (C–OH), 1026.

^1H and ^{13}C NMR data are given in Tables 5 and 6. The thermotropic behaviour is shown in Table 1.

2,3,7,8,12,13,17,18-Octakis(hydroxyalkylthio)-5,10,15,20-tetraazaporphyrin **4a–d**

3a–d (3 mmol) were stirred in 100 ml hot (80 °C) acetic acid for 30 min, and the demetallations were controlled by VIS spectroscopy. The violet solutions were added to 500 ml distilled water. The products were filtered and refluxed in 200 ml 5% aqueous Na₂CO₃ solution for 5 min. The filtered products were boiled in 200 ml 1% methanolic KOH to saponify partly formed acetic ester. The products were precipitated with distilled water, filtered and washed with distilled water and then freeze-dried. Purification of the violet microcrystalline products were carried out as described for **3a–d** by chromatography.

4a. (Yield 2.45 g, 79%), $\lambda_{\text{max}}(\text{THF})/\text{nm}$ 349 ($\epsilon/\text{dm}^3 \text{ mol}^{-1} \text{ cm}^{-1}$ 44 100), 511 (20 800), 641 (26 000), 712 (34 100); $\nu_{\text{max}}/\text{cm}^{-1}$ 3350br (OH), 3293w (NH), 2926 and 2854 (CH), 1050 (C–OH), 1013.

4b. (Yield 3.45 g, 84%), $\lambda_{\text{max}}(\text{THF})/\text{nm}$ 349 ($\epsilon/\text{dm}^3 \text{ mol}^{-1} \text{ cm}^{-1}$ 44 100), 511 (20 800), 641 (26 000), 712 (34 100); $\nu_{\text{max}}/\text{cm}^{-1}$

Table 7 ¹H NMR data of the compounds 6–7 (δ ; 360 MHz; DCCl₃)

Compound correlation	6a	6b	6c	6d	7a	7b	7c	7d
(16 H, t, SCH ₂)	4.2	4.1	4.1	4.0	4.2	4.1	4.1	4.1
(16 H, m, CH ₂)	2.25	1.95	1.9	1.9	2.3	1.9	1.9	1.9
(32 H, m, 2CH ₂)		1.7–1.6	1.7–1.5	1.7–1.5		1.7–1.6	1.7–1.5	1.7–1.5
(48 H, m, 3CH ₂)			1.4–1.1				1.4–1.2	
(96 H, m, 6CH ₂)				1.4–1.1				1.4–1.1
(16 H, m, CH ₂)		1.4				1.4		
(16 H, t, OCH ₂)	4.3	4.2	4.2	4.15	4.45	4.1	4.1	4.1
(8 H, d, OC–CH=)	6.0	6.3	6.3	6.2	5.8	6.2	6.2	6.25
(8 H, d, =CH–Ar)	7.15	7.55	7.6	7.6	7.1	7.5	7.5	7.6
(16 H, d, Ar–H)	7.2	7.45	7.5	7.4	6.95	7.35	7.4	7.4
(16 H, d, Ar–H) ^a	6.7	6.9	6.9	6.8	6.6	6.75	6.8	6.8
(24 H, s, OMe)	3.8	3.75	3.8	3.75	3.8	3.7	3.75	3.75
(2 H, s, NH)					–1.5	–1.2	–1.1	–1.1

^a Protons close to the methoxy group.

3360br (OH), 3292w (NH), 2931 and 2857 (CH), 1056 (C–OH), 1026.

4c. (Yield 3.88 g, 81%), λ_{\max} (THF)/nm 349 ($\epsilon/\text{dm}^3 \text{ mol}^{-1} \text{ cm}^{-1}$ 44 100), 511 (20 800), 641 (26 000), 712 (34 100); $\nu_{\max}/\text{cm}^{-1}$ 3355br (OH), 3289w (NH), 2926 and 2854 (CH), 1057 (C–OH), 1029.

4d. (Yield 4.64 g, 80%), λ_{\max} (THF)/nm 349 ($\epsilon/\text{dm}^3 \text{ mol}^{-1} \text{ cm}^{-1}$ 44 100), 511 (20 800), 641 (26 000), 712 (34 100); $\nu_{\max}/\text{cm}^{-1}$ 3360br (OH), 3289w (NH), 2920 and 2853 (CH), 1061 (C–OH), 1019.

¹H and ¹³C NMR data are given in Tables 5 and 6. The thermotropic behaviour is shown in Table 1.

2,3,7,8,12,13,17,18-Octakis(hydroxyalkylthio)-5,10,15,20-tetraazaporphyrinatocopper 5a–d

4a–d (1.5 mmol) and copper acetylacetonate (1.5 mmol, 393 mg) were refluxed in 50 ml methanol for 2 h, and the metallation was controlled by VIS-spectroscopy. The cold suspensions were added to 100 ml 5% aqueous NH₄Cl solution and filtered. The products were washed with distilled water and purified as described for **3a–d** by chromatography.

5a. (Yield 1.56 g, 95%), (Found: C, 43.8; H, 5.2. C₄₀H₅₆N₈O₈S₈Cu requires C, 44.0; 51%; λ_{\max} (THF)/nm 361 ($\epsilon/\text{dm}^3 \text{ mol}^{-1} \text{ cm}^{-1}$ 41 000), 502 (14 600), 668 (52 500); $\nu_{\max}/\text{cm}^{-1}$ 3345br (OH), 2921 and 2875 (CH), 1050 (C–OH), 1029sh.

5b. (Yield 2.11 g, 98%), (Found: C, 53.6; H, 7.4. C₆₄H₁₀₄N₈O₈S₈Cu requires C, 53.6; H, 7.3%; λ_{\max} (THF)/nm 361 ($\epsilon/\text{dm}^3 \text{ mol}^{-1} \text{ cm}^{-1}$ 41 000), 502 (14 600), 668 (52 500); $\nu_{\max}/\text{cm}^{-1}$ 3344br (OH), 2932 and 2857 (CH), 1050 (C–OH), 1034sh.

5c. (Yield 2.39 g, 96%), (Found: C, 58.0; H, 8.2. C₈₀H₁₃₄N₈O₈S₈Cu requires C, 57.95; H, 8.3%; λ_{\max} (THF)/nm 361 ($\epsilon/\text{dm}^3 \text{ mol}^{-1} \text{ cm}^{-1}$ 41 000), 502 (14 600), 668 (52 500); $\nu_{\max}/\text{cm}^{-1}$ 3345br (OH), 2930 and 2856 (CH), 1052 (C–OH), 1037sh.

5d. (Yield 2.72 g, 91%), (Found: C, 62.6; H, 9.3. C₁₀₄H₁₈₂N₈O₈S₈Cu requires C, 62.3; H, 9.2%; λ_{\max} (THF)/nm 361 ($\epsilon/\text{dm}^3 \text{ mol}^{-1} \text{ cm}^{-1}$ 41 000), 502 (14 600), 668 (52 500); $\nu_{\max}/\text{cm}^{-1}$ 3346br (OH), 2924 and 2853 (CH), 1050 (C–OH), 1038sh.

The thermotropic behaviour is shown in Table 1.

Magnesium-, metal-free-, copper-2,3,7,8,12,13,17,18-octakis[(4-methoxycinnamoyl)oxyalkylthio]tetraazaporphyrins 6a–d, 7a–d, 8a–d

Freeze-dried **3a–d**, **4a–d** or **5a–d** (0.5 mmol), dicyclohexylcarbodiimide (12 mmol), 4-methoxycinnamic acid (12 mmol) and toluene-*p*-sulfonic acid (0.5 mmol) were stirred in 50 ml dry pyridine. The progress of the reactions was followed by TLC on silica using toluene as eluent. After *ca.* one day for **6a**, **7a**, **8a** and up to seven days for **6d**, **7d**, **8d** the reactions were completed. 1 ml acetic acid was added to the suspensions before storage in a refrigerator over night. The suspensions were filtered, filtrates

concentrated and the products precipitated by adding 50 ml 10% aqueous Na₂CO₃ solution. The precipitates were isolated by centrifugation and washed several times with distilled water. The blue products were purified by column chromatography on silica using toluene or toluene–acetic ester 9:1 for **6a**, **7a**, **8a** as eluent. Residues of small amounts of hepta-esterified by-products in the long chain derivatives **6c,d**, **7c,d** and **8c,d** could be separated by preparative HPLC using a Merck LiChrosorb Si 60 (7 μm), 250–25 column and toluene as mobile phase. The flow-rate was 39 ml min^{–1} and the injection volume 10 ml by product concentrations of around 2 mg ml^{–1}.

6a. (Yield 0.81 g, 69%), λ_{\max} (THF)/nm 226 ($\epsilon/\text{dm}^3 \text{ mol}^{-1} \text{ cm}^{-1}$ 11 4000), 309 (189 000), 376 (51 000), 673 (4900); $\nu_{\max}/\text{cm}^{-1}$ 1705 (C=O), 1632 (C=C_{olef}), 1252 and 1028 (C–O–C).

6b. (Yield 0.96 g, 72%), λ_{\max} (THF)/nm 226 ($\epsilon/\text{dm}^3 \text{ mol}^{-1} \text{ cm}^{-1}$ 114 000), 309 (189 000), 376 (51 000), 673 (4900); $\nu_{\max}/\text{cm}^{-1}$ 1708 (C=O), 1631 (C=C_{olef}), 1251 and 1030 (C–O–C).

6c. (Yield 1.15 g, 79%), λ_{\max} (THF)/nm 226 ($\epsilon/\text{dm}^3 \text{ mol}^{-1} \text{ cm}^{-1}$ 114 000), 309 (189 000), 376 (51 000), 673 (4900); $\nu_{\max}/\text{cm}^{-1}$ 1710 (C=O), 1636 (C=C_{olef}), 1252 and 1030 (C–O–C).

6d. (Yield 1.13 g, 70%), λ_{\max} (THF)/nm 226 ($\epsilon/\text{dm}^3 \text{ mol}^{-1} \text{ cm}^{-1}$ 114 000), 309 (189 000), 376 (51 000), 673 (4900); $\nu_{\max}/\text{cm}^{-1}$ 1711 (C=O), 1635 (C=C_{olef}), 1252 and 1030 (C–O–C).

7a. (Yield 0.98 g, 85%), λ_{\max} (THF)/nm 226 ($\epsilon/\text{dm}^3 \text{ mol}^{-1} \text{ cm}^{-1}$ 118 000), 309 (199 000), 363 (50 000), 517 (23 000), 639 (29 000), 711 (38 000); $\nu_{\max}/\text{cm}^{-1}$ 1705 (C=O), 1632 (C=C_{olef}), 1252 and 1028 (C–O–C).

7b. (Yield 1.09 g, 82%), λ_{\max} (THF)/nm 226 ($\epsilon/\text{dm}^3 \text{ mol}^{-1} \text{ cm}^{-1}$ 118 000), 309 (199 000), 363 (50 000), 517 (23 000), 639 (29 000), 711 (38 000); $\nu_{\max}/\text{cm}^{-1}$ 1708 (C=O), 1631 (C=C_{olef}), 1251 and 1030 (C–O–C).

7c. (Yield 1.11 g, 77%), λ_{\max} (THF)/nm 226 ($\epsilon/\text{dm}^3 \text{ mol}^{-1} \text{ cm}^{-1}$ 118 000), 309 (199 000), 363 (50 000), 517 (23 000), 639 (29 000), 711 (38 000); $\nu_{\max}/\text{cm}^{-1}$ 1710 (C=O), 1636 (C=C_{olef}), 1252 and 1030 (C–O–C).

7d. (Yield 1.14 g, 71%), λ_{\max} (THF)/nm 226 ($\epsilon/\text{dm}^3 \text{ mol}^{-1} \text{ cm}^{-1}$ 118 000), 309 (199 000), 363 (50 000), 517 (23 000), 639 (29 000), 711 (38 000); $\nu_{\max}/\text{cm}^{-1}$ 1711 (C=O), 1635 (C=C_{olef}), 1252 and 1030 (C–O–C).

8a. (Yield 0.91 g, 76%), (Found: C, 60.7; H, 5.4; N, 4.9; O, 16.2; S, 10.9. C₁₂₀H₁₂₀N₈O₂₄S₈Cu requires C, 60.6; H, 5.1; N, 4.7; O, 16.15; S, 10.8%; λ_{\max} (THF)/nm 225 ($\epsilon/\text{dm}^3 \text{ mol}^{-1} \text{ cm}^{-1}$ 134 000), 309 (197 000), 361 (48 000), 503 (17 000), 669 (5900); $\nu_{\max}/\text{cm}^{-1}$ 1709 (C=O), 1634 (C=C_{olef}), 1258 and 1027 (C–O–C).

8b. (Yield 1.00 g, 74%), (Found: C, 63.6; H, 6.3; N, 4.4; O, 14.3; S, 9.5. C₁₄₄H₁₆₈N₈O₂₄S₈Cu requires C, 63.7; H, 6.2; N, 4.1; O, 14.1; S, 9.45%; λ_{\max} (THF)/nm 225 ($\epsilon/\text{dm}^3 \text{ mol}^{-1} \text{ cm}^{-1}$ 134 000), 309 (197 000), 361 (48 000), 503 (17 000), 669 (5900); $\nu_{\max}/\text{cm}^{-1}$ 1707 (C=O), 1635 (C=C_{olef}), 1254 and 1031 (C–O–C).

8c. (Yield 1.13 g, 77%), (Found: C, 65.6; H, 7.0; N, 4.1; O, 12.8; S, 8.9. C₁₆₀H₁₉₈N₈O₂₄S₈Cu requires C, 65.4; H, 6.8; N, 3.8; O, 13.1; S, 8.7%; λ_{\max} (THF)/nm 225 ($\epsilon/\text{dm}^3 \text{ mol}^{-1} \text{ cm}^{-1}$

134 000), 309 (197 000), 361 (48 000), 503 (17 000), 669 (5900); $\nu_{\max}/\text{cm}^{-1}$ 1710 (C=O), 1635 (C=C_{olef}), 1256 and 1031 (C–O–C). **8d**. (Yield 1.11 g, 68%), (Found: C, 67.8; H, 7.7; N, 3.6; S, 7.8. C_{18.4}H_{24.6}N₈O_{2.4}S₈Cu requires C, 67.5; H, 7.6; N, 3.4; S, 7.8%); $\lambda_{\max}(\text{THF})/\text{nm}$ 225 ($\epsilon/\text{dm}^3 \text{ mol}^{-1} \text{ cm}^{-1}$ 134 000), 309 (197 000), 361 (48 000), 503 (17 000), 669 (5900); $\nu_{\max}/\text{cm}^{-1}$ 1708 (C=O), 1636 (C=C_{olef}), 1253 and 1032 (C–O–C).

The ¹H NMR data of **6a–d** and **7a–d** are illustrated in Table 7 and the thermotropic behaviours of **6a–d–8a–d** in Table 1.

Acknowledgements

We thank Professor D. Kreysig for activities to start this project and the Volkswagen-Foundation for financial support under grant No. I/65908.

References

- 1 D. Wöhrle and D. Meissner, *Adv. Mater.*, 1991, **3**, 129.
- 2 J. J. Simon and H. J. Andre, *Molecular Semiconductors*, Springer-Verlag, Berlin, 1985, and references cited therein.
- 3 D. Wöhrle, D. Schlettwein, G. Schnurpfeil, G. Schneider, E. Karmann, T. Yoshida and M. Kaneko, *Polym. Adv. Technol.*, 1995, **6**, 317.
- 4 B. Tieke, *Adv. Mater.*, 1990, **2**, 222.
- 5 G. Schneider, D. Wöhrle, W. Spiller, J. Stark and G. Schulz-Ekloff, *Photochem. Photobiol.*, 1994, **60**/4, 333.
- 6 T. J. Dougherty, *Adv. Photochem.*, 1992, **17**, 275.
- 7 M. Shopova, D. Wöhrle, N. Stoichkova, A. Milev, V. Mantareva, S. Müller, K. Kcsabov and K. Georgiev, *J. Photochem. Photobiol. B*, 1994, **23**, 35.
- 8 M. Ehrl, F. W. Deeg, C. Bräuchle, O. Frank, A. Sobbi, G. Schulz-Ekloff and D. Wöhrle, *Chem. Mater.*, 1994, **6**, 3.
- 9 *Phthalocyanines, Properties and Applications*, eds. C. C. Leznoff and A. B. P. Lever, VCH, New York, 1989–1993, vols. 1–3, and references cited therein.
- 10 D. Wöhrle, *Chimia*, 1991, **45**, 307.
- 11 G. A. Ozin, *Adv. Mater.*, 1992, **4**, 10, 612.
- 12 H. Ringsdorf, B. Schlarb and J. Venzmer, *Angew. Chem.*, 1988, **100**, 117.
- 13 J.-M. Lehn, 1988, *Angew. Chem.*, **100**, 91.
- 14 R. D. George and A. W. Snow, *Chem. Mater.*, 1994, **6**, 1587.
- 15 F. Lelj, G. Morelli, G. Ricciardi, A. Roviello and A. Sirigu, *Liq. Cryst.*, 1992, 941.
- 16 J. Simon and C. Sirlin, *Pure Appl. Chem.*, 1989, **61**(9), 1625.
- 17 P. Roisin, J. D. Wright, R. J. M. Nolte, O. E. Sielcken and S. C. Thorpe, *J. Mater. Chem.*, 1992, **2**(1), 131.
- 18 R. J. M. Nolte and W. Drenth, *NATO ASI Ser., Ser. E*, 206 (*Inorg. Organomet. Polym. Spec. Prop.*), 1992, pp. 223–229.
- 19 M. Hanack and M. Lang, *Adv. Mater.*, 1994, **6**(11), 819–33.
- 20 P. G. Schouten, J. M. Warman, M. P. de Haas, C. F. van Nostrum, G. H. Gelinck, R. J. M. Nolte, M. J. Copyn, J. W. Zwikker, M. K. Engel, M. Hanack, Y. H. Chang and W. T. Ford, *J. Am. Chem. Soc.*, 1994, **116**, 6880.
- 21 P. L. Egerton, E. Pitts and A. Reiser, *Macromolecules*, 1981, **14**, 95.
- 22 C. Mertesdorf, H. Ringsdorf and J. Stumpe, *Liq. Cryst.*, 1991, **9**(3), 337.
- 23 S. Kurihara and T. Nonaka, *Mol. Cryst. Liq. Cryst.*, 1994, **238**, 39.
- 24 A. K. Sobbi, D. Wöhrle and D. Schlettwein, *J. Chem. Soc., Perkin Trans. 2*, 1993, **2**, 481.
- 25 C. J. Schramm and B. M. Hoffman, *Inorg. Chem.*, 1980, **19**, 383.
- 26 J. Fitzgerald, W. Taylor and H. Owen, *Synthesis*, 1991, 686.
- 27 C. S. Velázquez, G. A. Fox, W. E. Broderick, K. A. Andersen, O. P. Anderson, A. G. M. Barrett and B. M. Hoffman, *J. Am. Chem. Soc.*, 1992, **114**, 7416.
- 28 K. Holmberg and B. Hansen, *Acta Chem. Scand., Ser. B*, 1979, **33**, 410.
- 29 H. Eichhorn, D. Wöhrle and M. Dogan, *Merck Spectrum*, 1995, **1**, 7.
- 30 J. F. Van der Pol, E. Neeleman, J. C. Van Miltenburg, J. W. Zwikker, R. J. M. Nolte and W. Drenth, *Macromolecules*, 1990, **23**(1), 155.
- 31 R. B. Frings and W. Schnabel, *Polym. Photochem.*, 1983, **325**, 3.
- 32 S. Kurihara, T. Ikeda and S. Tazuke, *Macromolecules*, 1991, **24**, 627.
- 33 H. Cackovic, J. Springer and F. W. Weigelt, *Prog. Colloid Polym. Sci.*, 1984, **69**, 134.
- 34 A. A. Lamola and N. J. Turro, *Energy Transfer and Organic Photochemistry*, Interscience Publishers, New York, London, Sydney, Toronto, 1969, p. 37.
- 35 N. Kobayashi, in *Phthalocyanines, Properties and Applications*, eds. C. C. Leznoff and A. B. P. Lever, VCH, New York, 1991, vol. 2, p. 109, and references cited therein.
- 36 J. Stumpe and K. Wolf, *Mol. Cryst. Liq. Cryst.*, submitted.
- 37 Y. Shindo, K. Horie and I. Mita, *J. Photochem.*, 1984, **26**, 185–192.
- 38 H. H. Perkampus, *UV-VIS-Spektroskopie und ihre Anwendungen*, Springer-Verlag, Berlin, 1986, pp. 145–167.
- 39 E. Lippert and W. Lüder, *J. Phys. Chem.*, 1962, **66**, 2430.
- 40 V. Ramesh and R. G. Weiss, *Mol. Cryst. Liq. Cryst.*, 1986, **135**, 13.
- 41 Y. Shindo, K. Horie and I. Mita, *Chem. Lett.*, 1983, 639.
- 42 J. L. R. Williams, S. Y. Farid, J. C. Doty, R. C. Daly, D. P. Specht, R. Searle, D. G. Borden, H. J. Chang and P. A. Martin, *Pure Appl. Chem.*, 1977, **49**, 523.
- 43 J. Stumpe, S. Grande, K. Wolf and G. Hempel, *Liq. Cryst.*, 1992, **11**, 175.
- 44 J. Stumpe, O. Zaplo, D. Kreysig, M. Niemann and H. Ritter, *Makromol. Chem.*, 1992, **193**, 1567.
- 45 G. M. J. Schmidt, *Solid State Photochemistry*, Verlag Chemie, Weinheim, 1976.
- 46 H.-J. Timpe and U. Müller, *J. Photochem.*, 1987, **36**, 331.
- 47 A. Davison and R. H. Holm, *Inorg. Synth.*, 1967, **10**, 8.

Paper 6/02738E

Received 19th April 1996

Accepted 21st May 1996